Throughput Analysis of SIC-Based Two-Device Slotted ALOHA with Feedback Over Nakagami-m Fading Channels

Daiki Fukui*, Yuhei Takahashi*, Guanghui Song†, Tomotaka Kimura*, Zilong Liu‡, and Jun Cheng*
* Department of Intelligent Information Engineering and Sciences, Doshisha University, Kyoto, 610-0321, Japan
(e-mail: {ctwk0108, cyjk1101}@mail4.doshisha.ac.jp tomkimur@mail.doshisha.ac.jp; jcheng@ieee.org)
† The State Key Laboratory of Integrated Services Networks, Xidian University, Xi'an 710071, China
(e-mail:songguanghui@xidian.edu.cn)
‡ School of Computer Science and Electronic Engineering, University of Essex, Colchester, CO4 3SQ, UK
(e-mail:zilong.liu@essex.ac.uk)

***Abstract*—Throughput analysis for successive interference cancellation-based two-device slotted ALOHA with feedback is studied over Nakagami-m fading channels. Explicit expressions for the state transition probabilities are derived for a Markov process, thus facilitating the computation of the throughput. Through optimization of the transmission probability, it is shown that the maximum throughput is achieved for a given code rate. Simulations verify the analytical results.**

I. Introduction

This paper studies a K_T-device slotted ALOHA (SA) communication system, where K_T devices communicate with an access point (AP). As a random access protocol, SA has been adopted in numerous commercial communication systems and standards [1]. The legacy research on SAs relied on a collision channel model assuming negligible noise and fading, whereby the sent packets can be decoded from single-packet slots.

In recent years, it has been shown that the SA throughput can be significantly enhanced by exploiting the transmission diversity and inter-slot successive interference cancellation (SIC) [2] [3]. In fading environments, the intra-slot SIC further boosts the slots' decoding capacity. As far as the Rayleigh channels are concerned, Clazzer et al. derived the average normalized throughput [4] and our previous work in [5] explored the converse bound and the maximum a posteriori (MAP) threshold for the SA throughput. However, due to the absence of real-time feedback message (i.e., ACK) for acknowledging the packet retrieval, redundant packets may be transmitted, resulting in reduced spectrum and energy efficiencies.

By leveraging the real-time feedback, throughput analysis for two- and three-device SA systems was performed in a collision channel model in [6]. Moreover, in Rayleigh fading channels, iterative decoding was applied to two-device SA involving both intra- and inter-slot SICs, followed by a throughput analysis employing a Markov process. In [7], maximum sum rate was achieved by concurrently optimizing the transmission probability and the encoding rate of the devices through simulations.

In this study, we further investigate the two-device SA systems by expanding our analysis from Rayleigh to Nakagami-m channels. We present the expressions for the state transition probabilities in the Markov process, aiming to facilitate the computation of the throughput within Nakagami-m fading context. Through an optimization of the transmission probability, we achieve maximum throughput at a given code rate.

II. SIC-Based SA with Feedback

This section provides an overview of SIC-based SA with feedback over general fading channels, along with an analysis of their asymptotic performance using a Markov process [7].

A. Random Uplink Transmission and Re-transmission

We examine a K_T-device SA system, in which each device (as well as AP), equipped with a single antenna, employs a shared code $\mathcal{C}$ at code rate R. This encoder could be a combination of a channel encoder and a high-order modulator. In the receiver, AP iteratively decodes between intra- and inter-slot SICs and feeds real-time confirmation messages, i.e., ACKs, back to the devices. Such a system was studied in [7] and is referred to as SIC-based K_T-device SA systems with feedback. One may refer to [7] for details.

We assume that each device possesses an individual message stream. Each message gets encoded into a codeword, known as a packet, using code $\mathcal{C}$. The complete transmission period is segmented into time slots, whereby each slot's duration is designed to accommodate the transmission of a single packet. Once a packet is transmitted successfully, the device refreshes its message stream in preparation to send a new packet. By assumption, the devices are synchronized in terms of symbols and slots.

In the context of SA, during time slot t, each device transmits or re-transmits its packet to AP with transmission probability p and at power P. AP attempts to retrieve the packets from the superimposed signal in slot t and residual signals from earlier slots j $(< t)$. At the end of decoding at time t, AP distributes ACK messages to the devices whose packets have been completely retrieved. The devices that have successfully received their ACKs will update their message stream with new packets in subsequent slot $t+1$.

B. Decoding Processing over Fading Channels

Decoding is carried out between the intra- and inter-slots.

1) Decoding within a Slot: Intra-Slot SIC: Consider a generic slot, e.g., slot t, at some point during decoding. For the sake of concise notation, we omit index t in this subsection. Assuming K $(\le K_{\mathrm{T}})$ devices are active and transmit their packets to the slot, the resultant superimposed signal in the slot is $\boldsymbol{y} = \sum_{k\in\mathcal{K}} h_k \boldsymbol{x}_k + \boldsymbol{z}$. Here, device k is active and has accessed the slot. Vector $\boldsymbol{x}_k \in \mathcal{C}$ represents its codeword (or packet) of code $\mathcal{C}$, having rate R and length n. Set $\mathcal{K}$ is the group of active devices that are currently transmitting packets to the slot with the size of the set being $|\mathcal{K}| = K$. Vector $\boldsymbol{z} \sim \mathcal{CN}(\boldsymbol{0}, \sigma^2 I)$ is an additive, circularly symmetric complex Gaussian (CSCG) noise with mean $\boldsymbol{0}$ and diagonal covariance matrix $\sigma^2 I$ with noise power σ^2 and identity matrix I. Channel coefficient h_k signifies the fading of the channel from active device k to AP during the slot, and it is kept constant for a slot and then altered for the next slot. Every device is subjected to the identical power limitation $\|\boldsymbol{x}_k\|^2/n \le P$, and the signal-to-noise ratio (SNR) of the signal received from active device k is given by $\gamma_k = P|h_k|^2/\sigma^2$.

The channel coefficients are independent and distributed identically [7]. In this work, we focus on that random variable (RV) $|h_k|$ is *Nakagami-m* distributed. Then RV γ_k is distributed according to a gamma distribution with probability density function (PDF) [8, Eq. (2.21)]

$$p(\gamma_k) = \frac{m^m}{\Gamma(m)\bar{\gamma}^m}\gamma_k^{m-1}e^{-\frac{m}{\bar{\gamma}}\gamma_k}, \quad \gamma_k > 0, \tag{1}$$

where $\Gamma(z)$ is the gamma function [9, Eq. (8.310.1)] and $\bar{\gamma} = \mathbb{E}(\gamma_k)$ is the average received SNR of the signal from each device. Specifically, when we take into account that $m = 1$, Eq. (1) reduces to an exponential distribution with associated amplitude $|h_k|$ following a Rayleigh distribution [7].

In a threshold-based decoding, the packet (codeword) $\boldsymbol{x}_k$ is successfully decoded if signal-to-interference-plus-noise ratio (SINR) η_k exceeds a certain threshold η_0, i.e.,

$$\Pr\{\text{packet } \boldsymbol{x}_k \text{ decoded}\} = \begin{cases} 0, & \eta_k > \eta_0, \\ 1, & \eta_k \le \eta_0, \end{cases}$$

where the threshold for the SNR satisfies with $R = \log_2(1+\eta_0)$ for code rate R.

Inside the slot, the interference is canncelled successively from received signal $\boldsymbol{y}$. This is known as *intra-slot SIC*. Without loss of generality, we assume $\gamma_1 > \gamma_2 > \cdots > \gamma_K$. In the first step, we decode $\boldsymbol{x}_1$ and remove $h_1\boldsymbol{x}_1$ from $\boldsymbol{y}$ if the decoding is successful. After $\boldsymbol{x}_1, \boldsymbol{x}_2, \ldots, \boldsymbol{x}_{k-1}$ are successfully decoded, at step k of SIC, the SINR is

$$\eta_k \triangleq \frac{P|h_k|^2}{\sigma^2 + \sum_{u=k+1}^{K} P|h_u|^2} = \frac{\gamma_k}{1+\sum_{u=k+1}^{K}\gamma_u}. \tag{2}$$

Packet $\boldsymbol{x}_k$ will be successfully decoded if $\eta_k > \eta_0$, and otherwise SIC will stop. Note that it is assumed that AP has full awareness of the channel state information.

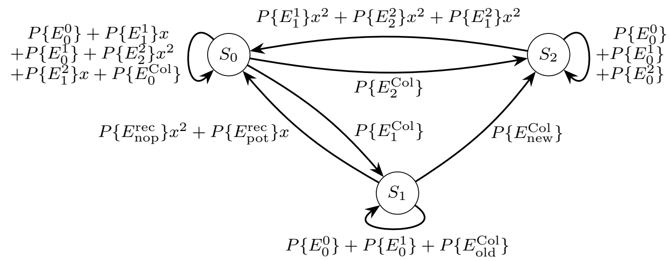

Fig. 1: State transition diagram of the Markov process for the two-device case [7].

A slot where AP manages to retrieve κ packets from $\boldsymbol{y}$ using the intra-slot SIC is defined as a *κ-recovery* slot. The remaining signal, containing $K-\kappa$ packets that have not been recovered, is known as a $(K-\kappa)$-collided residual signal of that slot. This residual signal is then stored in a residual buffer, awaiting further processing.

2) Decoding between Slots: Inter-Slot SIC: Following an intra-slot SIC at slot t, if a recovered packet in the slot is identified as a re-transmission, the interference from its duplicates will be canceled from the associated residual signal(s) at earlier slots j $(< t)$ within the residual buffer. This enables further intra-slot SICs on these signals. The process is repeated until decoding is no longer possible for any packets in the buffer. Upon successful recovery of packets, AP sends ACKs to the respective devices.

C. Markov Process of Two-Device SA [6] [7]

This subsection examines the modeling of the SIC-based two-device SA with feedback as a Markov process.

Before describing states of the residual buffer, it is essential to define *potentially-decodable* (PD) packet. In the context of a residual signal, an unrecovered packet $\boldsymbol{x}_k$ qualifies as PD when its SNR satisfies $\gamma_k > \eta_0$. In a two-collision scenario, the residual signal can have zero, one, or two PD packets. In scenario involving a single-packet slot (one-collision), storing an un-decodable packet to the buffer is redundant, hence no PD packets are present.

The decoding processing between intra- and inter-slot SICs can be modeled as a Markove process. The state set of the two-device residual signal buffer is defined by $\mathcal{S} = \{S_0, S_1, S_2\}$. State S_0 indicates that no PD packet exit in the buffer, and state S_1 (S_2) indicates that one (two) PD packets exit(s).

Let $\Pr\{s_t, d_t | s_{t-1}\}$ be a probability of a state transition from s_{t-1} to s_t and let d_t packets be recovered along with this state transition. A state-transition probability polynomial is defined as $p_{s_{t-1},s_t}(x) \triangleq \sum_{d=0}^{2}\Pr\{s_t, d_t = d | s_{t-1}\}x^d$, which indicate the expected number of recovered packets in the transition [6]. A state transition is triggered by decoding in the current slot t. The events that occur in the decoding of slot t are described in Table I.

Let us explain the state transitions, for example, from $s_{t-1} = S_2$ to $s_t = S_0$. During the decoding of slot t, three scenarios can initiate this transition. Firstly, if two packets are decodable in a two-collision (event E_2^2), their replicas are eliminated from the previous residual signals, and no residual signal exits at slot t. Consequently, the buffer state updates to

TABLE I: Events Occurring in the Current Slot [7]

event	interpretation
E_m^n	n active devices with m-recovery, ($m \le n$, $n = 0, 1, 2$)
$E_{\text{nop}}^{\text{rec}}$	a packet is recovered, whose replica in the buffer is not PD
$E_{\text{pot}}^{\text{rec}}$	only a packet is recovered, whose replica in the buffer is PD
E_j^{Col}	j PD packets in 2-collision ($j = 0, 1, 2$)
$E_{\text{new}}^{\text{Col}}$	two-collision occurs with a new PD packet
$E_{\text{old}}^{\text{Col}}$	two-collision occurs without a new PD packet

$s_t = S_0$. Secondly, if one of two packets in a two-collision event (event E_1^2) is decodable, its replica is removed from the previous residual signals. The other packet is then decoded due to PD in residual signals, leading to a buffer state of $s_t = S_0$. The third scenario occurs when a packet is decodable in a one-collision (event E_1^1), resulting in the buffer state transitioning to $s_t = S_0$. The probabilities for these transitions are given by

$$\begin{aligned}&\Pr\{s_t = S_0, d_t = 0|s_{t-1} = S_2\} = 0\\&\Pr\{s_t = S_0, d_t = 1|s_{t-1} = S_2\} = 0\\&\Pr\{s_t = S_0, d_t = 2|s_{t-1} = S_2\} = P\{E_2^2\} + P\{E_1^2\} + P\{E_1^1\}.\end{aligned}$$

The polynomial representing the state-transition probability is $p_{s_{t-1}=S_2, s_t=S_0}(x) = P\{E_2^2\}x^2 + P\{E_1^2\}x^2 + P\{E_1^1\}x^2$. State-transition polynomial matrix is then expressed in (3) [7].

The first-order derivative $\mathrm{d}p_{s',s}(x)/\mathrm{d}x$ evaluated at $x = 1$ indicates the expected number of packets retrieved during the transition from state s' to state s. Consequently, matrix $P'(x = 1) = \mathrm{d}P(x)/\mathrm{d}x|_{x=1}$, which measures number of packets during transition, is then

$$\mathrm{P}'(1) = \begin{pmatrix} P\{E_1^1\} + P\{E_1^2) + 2P(E_2^2\} & 0 & 0 \\ 2P\{E_{\text{nop}}^{\text{rec}}\} + P\{E_{\text{pot}}^{\text{rec}}\} & 0 & 0 \\ 2P\{E_1^1\} + 2P\{E_2^2\} + 2P\{E_1^2\} & 0 & 0 \end{pmatrix}. \quad (4)$$

Let a stationary distribution of the Markov process be $\boldsymbol{w} = (w_0, w_1, w_2)^{\mathrm{T}}$, such that $\boldsymbol{w}^{\mathrm{T}} P(x = 1) = \boldsymbol{w}^{\mathrm{T}}$ and $\boldsymbol{w}^{\mathrm{T}}\mathbf{1} = 1$, where $\mathbf{1} = (1, 1, 1)^{\mathrm{T}}$. The normalized throughput of the two-device SA with SICs and feedback, as $t \to \infty$, is given by

$$T(p, R, \bar{\gamma}, m) = \boldsymbol{w}^{\mathrm{T}} P'(1)\mathbf{1} \quad (5)$$

which represents the average number of packets decoded successfully per time slot.

III. Event Probabilities over Nakagami-m Fading

In this section, we provide explicit expressions for the event probabilities in Table I over the Nakagami-m channels with m being an integer, as commonly noted in the literature.

A. Preliminary

To simplify the notation, we reformulate (1) as $p(\gamma_j) = a\gamma_j^{m-1}e^{-c\gamma_j}$, where $a = \frac{m^m}{\Gamma(m)\bar{\gamma}^m}$ and $c = \frac{m}{\bar{\gamma}}$. It follows that, for the PDF, $\int_0^\infty p(\gamma_j)\mathrm{d}\gamma_j = ac^{-m}(m-1)! = 1$.

For the computation of the event probabilities, it is necessary to evaluate the lower and upper incomplete gamma functions as series expansions [9, Eq. 8.352.1] [9, Eq. 8.352.4], considering m as a positive integer.

$$\gamma(m, x) \triangleq \int_0^x t^{m-1}e^{-t}\mathrm{d}t = (m-1)!(1 - e^{-x}\sum_{k=0}^{m-1}\frac{x^k}{k!}). \quad (6)$$

$$\Gamma(m, x) \triangleq \int_x^\infty t^{m-1}e^{-t}\mathrm{d}t = (m-1)!e^{-x}\sum_{k=0}^{m-1}\frac{x^k}{k!}. \quad (7)$$

In addition, the (complete) gamma function defined below is related to the factorial by [9, Eqs. (8.310.1) and (8.321.1)]

$$\Gamma(m) \triangleq \int_0^\infty t^{m-1}e^{-t}\mathrm{d}t = (m-1)!. \quad (8)$$

B. Probabilities of E_m^n

We are now ready to compute the probabilities of events in Table I. Initially, we evaluate $P\{E_2^2\}$. Considering a superimposed signal from two packets, the probability of both packets being successfully decoded is $\Pr\{\frac{\gamma_1}{1+\gamma_2} > \eta_0, \gamma_2 > \eta_0\}$ under the assumption that $\gamma_1 > \gamma_2$. There is also a scenario where $\gamma_1 < \gamma_2$. Furthermore, the probability of both devices are active in the same slot is p^2. Consequently, the probability for event E_2^2 can be described as follows:

$$\begin{aligned}P\{E_2^2\} =& 2p^2\Pr\{\frac{\gamma_1}{1+\gamma_2} > \eta_0, \gamma_2 > \eta_0\}\\=& 2p^2\int_{\eta_0}^\infty p(\gamma_2)\int_{\eta_0(1+\gamma_2)}^\infty p(\gamma_1)\mathrm{d}\gamma_1\mathrm{d}\gamma_2. \quad (9)\end{aligned}$$

where the integral with respect to γ_1 is

$$\begin{aligned}&\int_{\eta_0(1+\gamma_2)}^\infty p(\gamma_1)\mathrm{d}\gamma_1 = ac^{-m}\Gamma(m, c(\eta_0(1+\gamma_2)))\\&= e^{-c\eta_0(1+\gamma_2)}\sum_{k_1=0}^{m-1}\frac{(c\eta_0)^{k_1}(1+\gamma_2)^{k_1}}{k_1!}\\&\overset{(a)}{=} e^{-c\eta_0(1+\gamma_2)}\sum_{k_1=0}^{m-1}\left(\frac{(c\eta_0)^{k_1}}{k_1!}\sum_{k_2=0}^{k_1}\binom{k_1}{k_2}\gamma_2^{k_2}\right). \quad (10)\end{aligned}$$

In (a) we use binomial expansion $(1+x)^n = \sum_{k=0}^n \binom{n}{k}x^k$. In (9), we then integrate with respect to γ_2

$$\begin{aligned}&\int_{\eta_0}^\infty p(\gamma_2)e^{-c\eta_0(1+\gamma_2)}\gamma_2^{k_2}\mathrm{d}\gamma_2\\&= ae^{-c\eta_0}\int_{\eta_0}^\infty \gamma_2^{m+k_2-1}e^{-c(1+\eta_0)\gamma_2}\mathrm{d}\gamma_2\\&= ae^{-c\eta_0}(c+c\eta_0)^{-(m+k_2)}\Gamma(m+k_2, c\eta_0(1+\eta_0)). \quad (11)\end{aligned}$$

Thus, the probability of the event E_2^2 is:

$$\begin{aligned}P\{E_2^2\} = 2p^2ae^{-c\eta_0}\sum_{k_1=0}^{m-1}\Bigg(\frac{(c\eta_0)^{k_1}}{k_1!}\\ \cdot\sum_{k_2=0}^{k_1}\binom{k_1}{k_2}(c+c\eta_0)^{-(m+k_2)}\Gamma(m+k_2, c\eta_0(1+\eta_0))\Bigg).\end{aligned}$$

$$P(x)=\begin{pmatrix} P\{E_0^0\}+P\{E_1^1\}x+P\{E_0^1\}+P\{E_2^2\}x^2+P\{E_1^2\}x+P\{E_0^{\rm Col}\} & P\{E_1^{\rm Col}\} & P\{E_2^{\rm Col}\} \\ P\{E_{\rm nop}^{\rm rec}\}x^2+P\{E_{\rm pot}^{\rm rec}\}x & P\{E_0^0\}+P\{E_0^1\}+P\{E_{\rm old}^{\rm Col}\} & P\{E_{\rm new}^{\rm Col}\} \\ P\{E_1^1\}x^2+P\{E_2^2\}x^2+P\{E_1^2\}x^2 & 0 & P\{E_0^0\}+P\{E_0^1\}+P\{E_0^2\} \end{pmatrix} \quad (3)$$

Likewise, the subsequent probabilities are as follows.

$$\begin{aligned} P\{E_1^2\} &= 2p^2\Pr\{\frac{\gamma_1}{1+\gamma_2}>\eta_0,\gamma_2<\eta_0\} \\ &=2p^2\int_0^{\eta_0}p(\gamma_2)\int_{\eta_0(1+\gamma_2)}^{\infty}p(\gamma_1)d\gamma_1 d\gamma_2 \\ &=2p^2ae^{-c\eta_0}\sum_{k_1=0}^{m-1}\Bigg(\frac{(c\eta_0)^{k_1}}{k_1!} \\ &\quad\cdot\sum_{k_2=0}^{k_1}\binom{k_1}{k_2}(c+c\eta_0)^{-(m+k_2)}\gamma(m+k_2,c\eta_0(1+\eta_0))\Bigg). \end{aligned}$$

$$\begin{aligned} P\{E_0^2\} &= 2p^2\Pr\{\gamma_2<\gamma_1<\eta_0(1+\gamma_2),0<\gamma_2<\infty\} \\ &=2p^2\int_0^{\infty}p(\gamma_2)\int_{\gamma_2}^{\eta_0(1+\gamma_2)}p(\gamma_1)d\gamma_1 d\gamma_2. \\ &=2p^2\sum_{k_1=0}^{m-1}\frac{(c)^{k_1}}{k_1!}a(2c)^{-(m+k_1)}\Gamma(m+k_1) \\ &\quad-2p^2ae^{-c\eta_0}\sum_{k_1=0}^{m-1}\Bigg(\frac{(c\eta_0)^{k_1}}{k_1!}\sum_{k_2=0}^{k_1}\binom{k_1}{k_2}(c+c\eta_0)^{-(m+k_2)} \\ &\quad\cdot\Gamma(m+k_2)\Bigg). \end{aligned}$$

Moreover, when a single packet is the only one received in the current slot, the probabilities are as follows:

$$\begin{aligned} P\{E_1^1\} &=2p(1-p)\Pr\{\gamma_1>\eta_0\}=2p(1-p)ac^{-m}\Gamma(m,c\eta_0) \\ P\{E_0^1\} &=2p(1-p)\Pr\{\gamma_1\le\eta_0\}=2p(1-p)ac^{-m}\gamma(m,c\eta_0) \\ P\{E_0^0\} &=(1-p)^2. \end{aligned}$$

C. Probabilities of $E_j^{\rm Col}$

In a similar manner, we determine the probabilities $P\{E_j^{\rm Col}\}$ for the existence of j PD packet(s) during a two-collision scenario, where $j=2,1,0$.

$$\begin{aligned} P\{E_2^{\rm Col}\} &= 2!p^2\Pr\{\gamma_2<\gamma_1<\eta_0(1+\gamma_2),\eta_0<\gamma_2\} \\ &=2!p^2\int_{\eta_0}^{\infty}p(\gamma_2)\int_{\gamma_2}^{\eta_0(1+\gamma_2)}p(\gamma_1)\mathrm{d}\gamma_1\mathrm{d}\gamma_2 \\ &=2p^2a\sum_{k_1=0}^{m-1}\frac{c^{k_1}}{k_1!}(2c)^{-(m+k_1)}\Gamma(m+k_1,2c\eta_0) \\ &\quad-2p^2ae^{-c\eta_0}\sum_{k_1=0}^{m-1}\Bigg(\frac{(c\eta_0)^{k_1}}{k_1!}\sum_{k_2=0}^{k_1}\binom{k_1}{k_2}(c+c\eta_0)^{-(m+k_2)} \\ &\quad\cdot\Gamma(m+k_2,c\eta_0(1+\eta_0))\Bigg). \end{aligned}$$

$$\begin{aligned} P\{E_1^{\rm Col}\} &= 2!p^2\Pr\{\eta_0<\gamma_1<\eta_0(1+\gamma_2),0<\gamma_2<\eta_0\} \\ &=2!p^2\int_0^{\eta_0}p(\gamma_2)\int_{\eta_0}^{\eta_0(1+\gamma_2)}p(\gamma_1)\mathrm{d}\gamma_1\mathrm{d}\gamma_2 \\ &=2p^2ac^{-m}e^{-c\eta_0}\gamma(m,c\eta_0)\sum_{k_1=0}^{m-1}\frac{(c\eta_0)^{k_1}}{k_1!} \\ &\quad-2p^2ae^{-c\eta_0}\sum_{k_1=0}^{m-1}\Bigg(\frac{(c\eta_0)^{k_1}}{k_1!}\sum_{k_2=0}^{k_1}\binom{k_1}{k_2}(c+c\eta_0)^{-(m+k_2)} \\ &\quad\cdot\gamma(m+k_2,c\eta_0(1+\eta_0))\Bigg). \end{aligned} \quad (12)$$

$$\begin{aligned} P\{E_0^{\rm Col}\} &=2!p^2\Pr\{\gamma_2<\gamma_1<\eta_0,0<\gamma_2<\eta_0\} \\ &=2p^2\int_0^{\eta_0}p(\gamma_2)\int_{\gamma_2}^{\eta_0}p(\gamma_1)\mathrm{d}\gamma_1\mathrm{d}\gamma_2 \\ &=2p^2a\sum_{k_1=0}^{m-1}\frac{c^{k_1}}{k_1!}(2c)^{-(m+k_1)}\gamma(m+k_1,2c\eta_0) \\ &\quad-2p^2e^{-c\eta_0}ac^{-m}\gamma(m,c\eta_0)\sum_{k_1=0}^{m-1}\frac{(c\eta_0)^{k_1}}{k_1!}. \end{aligned}$$

D. Probabilities of $P\{E_{\rm pot}^{\rm rec}\}$, $P\{E_{\rm nop}^{\rm rec}\}$, $P\{E_{\rm new}^{\rm Col}\}$, $P\{E_{\rm old}^{\rm Col}\}$

To illustrate, take the event $E_{\rm pot}^{\rm rec}$ as an example. This event happens when a) a packet from the current slot is successfully recovered, and b) this recovered packet turns out to be a PD replica within the buffer. If condition (a) is met, then condition (b) will occur with a probability of 1/2. Consequently [7],

$$P\{E_{\rm pot}^{\rm rec}\}=(P\{E_1^1\}+P\{E_1^2\})/2.$$

Likewise, the other probabilities listed in Table I are detailed in the same reference [7]

$$\begin{aligned} P\{E_{\rm nop}^{\rm rec}\} &=(P\{E_1^1\}+P\{E_1^2\})/2+P\{E_2^2\} \\ P\{E_{\rm new}^{\rm Col}\} &=P\{E_1^{\rm Col}\}/2+P\{E_2^{\rm Col}\} \\ P\{E_{\rm old}^{\rm Col}\} &=P\{E_1^{\rm Col}\}/2+P\{E_0^{\rm Col}\}. \end{aligned}$$

Remark 1: It is a recognized fact that the gamma distribution, as shown in (1), simplifies to an exponential distribution when $m=1$. Consequently, the event probabilities calculated in this work correspond to those reported in [7], where the channel fading is a Rayleigh distribution, that is, $m=1$, for the channel amplitude $|h_k|$. □

Remark 2: It should be noted that the intra-slot SIC is typically utilized for managing, for example, two-collision scenarios in most systems [10], primarily due to increased interference from multiple devices, increased cumulative error in the SIC, and extensive computational complexity. Consequently, in configurations involving multiple devices, it is advisable to focus solely on two-collision decoding. Our analysis can be adapted to accommodate a multi-device configuration

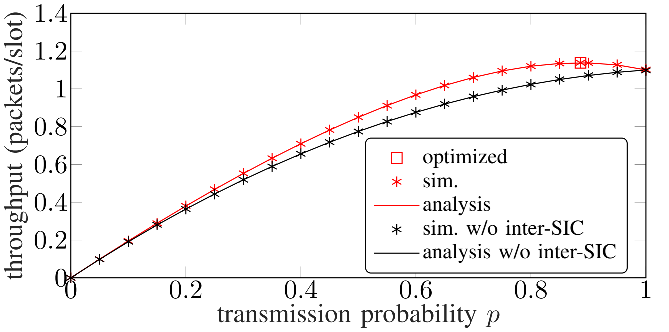

Fig. 2: The normalized throughput under $R = 1.2$, $m = 5$, and $\bar{\gamma} = 10$ dB. The maximum throughput is $T^* = 1.1377$ packet/slot obtained at $p^* = 0.8863$. Also, the throughput without the inter-slot SIC is shown.

that incorporates two-collision decoding in the current slot while disregarding, for example, five or more collisions. The resultant number of states is moderate and acceptable. □

E. Optimization of Transmission Probability p

Prior to concluding this section, we aim to optimize transmission probability p. This optimization ensures that the normalized throughput (5) is maximized, for given code rate R, average received SNR $\bar{\gamma}$, and Nakagami parameter m.

$$\begin{aligned} &\underset{0<p\leq 1}{\text{maximize}} \quad T(p, R, \bar{\gamma}, m). \\ &\text{subject to} \quad R, \bar{\gamma}, m \text{ are constant.} \end{aligned} \tag{13}$$

IV. Numerical and Simulation Results

In this section, we present the numerical results for the normalized throughput (5) and its maximum value achieved by optimizing the transmission probability. Additionally, we conduct computer simulations to verify our analytical results.

Figure 2 displays the numerical results for the throughput of (5) with code rate $R = 1.2$, average received SNR $\bar{\gamma} = 10$ dB, and Nakagami parameter $m = 5$. For comparison purposes, simulation results ranging from $p = 0$ to 1 in increments of 0.05 are also presented with the number of slots $n_s = 10^6$. The two results are in agreement. Moreover, the optimization problem outlined in (13) was addressed using the golden-section search technique. The maximum throughput, $T^* = 1.1377$ (packets/slot), was obtained at $p^* = 0.8863$, consistent with both the numerical analysis and simulation results. Also in Fig. 2, we give the results of two-device SA with the intra-slot SIC only. Without the inter-slot SIC, the throughput is represented as $T = \mathrm{d}p_{S_0,S_0}(x)/\mathrm{d}x|_{x=1} = P\{E_1^1\} + P\{E_1^2) + 2P(E_2^2\}$, which is entry $(P'(1))_{(0,0)}$ of (4). Obviously, the inter-slot SIC improves the throughput.

With the same parameters as Fig. 2, we give the throughputs for $m = 1, 3$, and 5 in Fig. 3. Our analysis results includes the previous ones [7], as a special case of $m = 1$.

Furthermore, with $R = 6.129$ and $\bar{\gamma} = 25$ dB, the same parameters as [7], we present the numerical, simulation, and optimized findings in Fig. 4 with $m = 1$. The optimized values are $p^* = 0.590$ and $T^* = 0.560$, which coincide with the findings of previous work [7]. In addition, the analytic throughput in the collision channel model [6] is shown, which is consistent with that of $m = 5$. This is expected, as

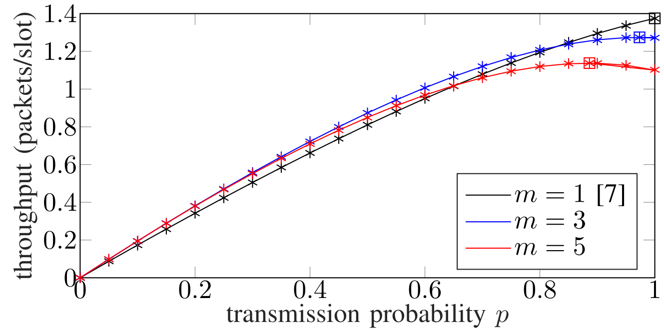

Fig. 3: The normalized throughput for $m = 1, 3$ and 5. Markers $*$ and □ indicate the simulation and optimize results. The specifications of the parameters are the same as in Fig. 2.

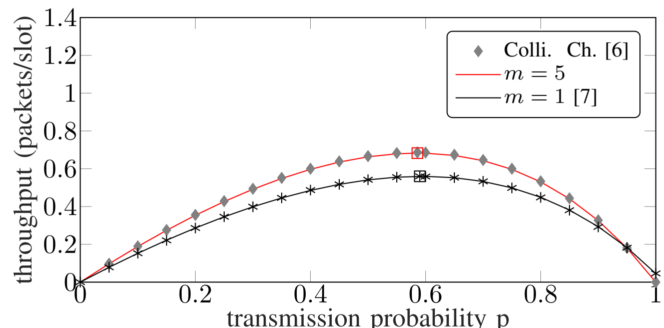

Fig. 4: The normalized throughputs ($m = 1$ and 5) with $R = 6.129$ and $\bar{\gamma} = 25$ dB. The optimal values for $m = 1$ are $p^* = 0.590$ and $T^* = 0.560$. Also, the analytic throughput in the collision channel model [6] is shown.

Nakagami-m fading approaches the behavior of a non-fading AWGN channel as m increases along with an elevated $\bar{\gamma}$ [8].

Finally, we present simulation outcomes for a limited range of slots in Fig. 5. As n_s increases, the throughputs approach their asymptotic values.

V. Conclusion

We have provided formulations for the state transition probabilities and this allows us to determine the analytical throughput for SIC-based two-device SA systems with feedback over Nakagami-m fading channels. By optimizing the transmission probability, the throughput at a given code rate is maximized. The extension of Nakagami-m to mixture gamma fading channel can be easily achieved.

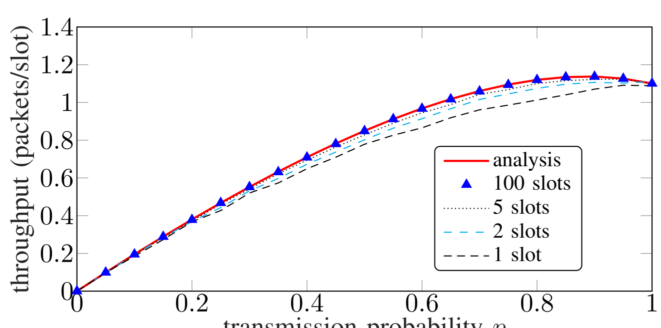

Fig. 5: Throughputs with the increment of number of slots in simulations. The specifications are the same as Fig. 2.

REFERENCES

[1] A. Munari, "Modern random access: An age of information perspective on irregular repetition slotted ALOHA," *IEEE Transactions on Communications*, vol. 69, no. 6, pp. 3572–3585, 2021.

[2] G. Liva, "Graph-based analysis and optimization of contention resolution diversity slotted ALOHA," *IEEE Transactions on Communications*, vol. 59, no. 2, pp. 477–487, 2011.

[3] E. Paolini, C. Stefanovic, G. Liva, and P. Popovski, "Coded random access: applying codes on graphs to design random access protocols," *IEEE Communications Magazine*, vol. 53, no. 6, pp. 144–150, 2015.

[4] F. Clazzer, E. Paolini, I. Mambelli, and Č. Stefanović, "Irregular repetition slotted ALOHA over the Rayleigh block fading channel with capture," in *IEEE International Conference on Communications (ICC)*, 2017, pp. 1–6.

[5] Y. Takahashi, G. Song, T. Kimura, and J. Cheng, "Irregular repetition slotted ALOHA over Rayleigh block fading channels: Bounds and threshold saturation via spatial coupling," *IEEE Access*, vol. 11, pp. 106 528–106 543, 2023.

[6] G. Song, K. Cai, Y. Chi, and J. Cheng, "Throughput analysis of interference cancellation-based random access with feedback," *IEEE Communications Letters*, vol. 22, no. 12, pp. 2423–2426, 2018.

[7] Z. Zhang, Y. Li, G. Song, C. Yuen, and Y. L. Guan, "Random NOMA with cross-slot successive interference cancelation packet recovery," *IEEE Wireless Communications Letters*, vol. 9, no. 7, pp. 1065–1069, 2020.

[8] M. K. Simon and M. S. Alouini, *Digital Communication over Fading Channels; 2nd ed.* Newark, NJ: Wiley, 2005.

[9] I. Gradshteyn and I. Ryzhik, "Table of integrals, series, and products," 2007. [Online]. Available: http://fisica.ciens.ucv.ve/~svincenz/TISPISGIMR.pdf

[10] N. Zhang, J. Wang, G. Kang, and Y. Liu, "Uplink nonorthogonal multiple access in 5G systems," *IEEE Communications Letters*, vol. 20, no. 3, pp. 458–461, 2016.